

Design of Boost Converter with PI & IP Controllers and PI Observer

G.V.S.Lakshmi¹, Dr.K.Rama Sudha²

¹ (PG Scholar, Dept. of Electrical Engineering, AUCE (A), Andhra University, INDIA)

² (Professor, Dept. of Electrical Engineering, AUCE(A), Andhra University, INDIA)

Corresponding Author: G.V.S.Lakshmi

Abstract: DC/DC boost converters are known for presenting highly nonlinear and non-minimum phase properties. A predesigned cascade controller and nested reduced-order proportional-integral observers (PIOs) are designed to maintain the desirable voltage regulation performance of the cascade controller for a dc/dc boost converter subject to reference input change, load change and input voltage variations. In the cascade controller design, the fast-inner current loop adopts proportional-integral control and the slow outer voltage loop employs integral-proportional control based on a linearized model at a single nominal operating point. Unified theoretical analysis is performed by applying singular perturbation theory, which confirms the desired approximation of the augmented system with the PIOs to the nominal closed-loop system using the cascade controller without accounting for the uncertainties.

The boost converter was tested via computer simulations using MATLAB under reference input change, load change and input voltage variations. The bode plot analysis of the boost converter is tabulated under load change, parametric uncertainties, and input voltage variations and observed that the system is more stable with proportional-integral observers (PIOs).

The boost converter is implemented using hardware components. The output voltage is obtained by giving the input through DC 12V battery and solar panel and observed that the output voltage is approximately equal to 2.5 times the input voltage in both the cases.

Keywords- Cascade control, DC-DC power converters, PI & IP controllers, PI observers, Stability.

Date of Submission: 17-02-2019

Date of acceptance: 03-03-2019

I. Introduction

To accommodate varying power requirements in a system and optimize energy efficiency, the voltage provided by a source can be stepped up or down using DC-DC power converters [1]. The generated dc voltage is usually low in amplitude and unexpected transient states often result from uncertain load variations. In such applications, it is required that the converters provide a highly regulated dc voltage under various system uncertainties, such as load change, parametric uncertainties, and input voltage variations.

In order to gain a deep understanding of the operation and designing aspects involved with conventional step-up converter, a mathematical model to accurately evaluate performance is developed in MATLAB environment. The circuit is evaluated using the model under varying operating conditions and parasitics. As a result, a better understanding of the issues involved in converter design for better performance is achieved. In this paper we have performed the stability analysis of the system and observed that the system is more stable for duty cycle $D=0.8$ and the system is more stable using cascade (PI & IP) Controllers along with PI observers rather than using only cascade controllers.

The same system is developed using hardware and the outputs were obtained in such a way that it is almost equal to 2.5 times the input.

II. Various control strategies

2.1. Pulse-width modulation

Pulse-width modulation (PWM), or pulse-duration modulation (PDM), is a way of describing a digital (binary/discrete) signal that was created through a modulation technique, which involves encoding a message into a pulsing signal. Although this modulation technique can be used to encode information for transmission, its main use is to allow the control of the power supplied to electrical devices, especially to inertial loads such as motors. In this paper, in order to generate the required pulse width modulation signal, the output signal is compared with the reference input signal.

2.2. P-I controller & I-P controller

The proportional-integral (P - I) is one of the conventional controllers and it has been widely used for the speed control of dc motor drives. The major features of the (P - I) controller are its ability to maintain a zero steady-state error to a step change in reference and its simple and straight-forward microprocessor implementation. On the other hand (P-I) controller has some disadvantages such as the undesirable speed overshoot, the sluggish response due to sudden change in load torque and the sensitivity to controller gains K_p , and K_i [4].

The (P - I) controller has a proportional as well as an integral term in the forward path. The integral controller has the property of making the steady-state error zero for a step change, although a (P - I) controller makes the steady-state error zero, it may take a considerable amount of time to accomplish this. The (I - P) controller[4] has the proportional in the feedback path and it acts like a feedback compensation. The (P - I) and (I - P) controllers have the same characteristic equations, and the zero introduced by the (P - I) controller is absent in the case of the (I-P) controller. Therefore, the overshoot in the speed, for a step change in the input reference $R(S)$, is expected to be smaller for the (I- P) control. Therefore, the response to a load disturbance is expected to be very similar for both (P - I) and (I - P) controllers.

2.3. Proportional Integral observer

Observers play a crucial role in control because some control methods require the accurate estimation of system to realize the closed loop control tasks. High-quality performance could be achieved through the estimation of unknown inputs affecting the system such as disturbances or model uncertainties. Beside the estimation of states and unknown inputs, observers are also able to increase the control performance[3].

Estimation of system states and unknown inputs based on the system input-output can be solved for linear system using Proportional-Integral-Observer. Because of non-efficiency of proportional observers in the presence of unknown input acting to the system, PI-Observer has been proposed to estimate unknown inputs[3]. Luenberger observer is widely used in classical control field because of its capability to estimate system states. This observer has two feedback loops to be designed. Both (the proportional and the integral loop) loops are used as feedback to reconstruct not only the system states but also the disturbances, unmodeled dynamics, or modelling errors as nonlinearities assumed as additive acting inputs.

A general model for a linear time invariant system with unknown inputs can be described as

$$\begin{aligned} \dot{x}(t) &= Ax(t) + Bu(t) + Nd(x,t) + E_g(x,t) \\ y(t) &= Cx(t) + h(t) \end{aligned} \quad (1)$$

with the state vector $x(t) \in R^n$, input vector $u(t) \in R^m$, measurement vector $y(t) \in R^r$, unknown input $d(x,t) \in R^1$, measurement noise $h(t) \in R$, and unmodeled dynamics $g(x,t) \in R^p$. Here the unknown input $d(x,t)$ and the input matrix N are used to model the additive unknown inputs. Depending on the design approach, knowledge about the dynamics of $d(x,t)$ is assumed (disturbance observer) or not assumed (Proportional-Integral observer). Matrices A , B , and C are assumed as known and of appropriate dimensions.

III. Performance of boost converter with controllers & observers

A Reliable dc/dc boost conversion stage is essential for various industrial applications, including renewable energy sources, because the generated dc voltage is usually low in amplitude and unexpected transient states often result from uncertain load variations. In such applications, it is required that the converters provide a highly regulated dc voltage under various system uncertainties, such as load change, parametric uncertainties, and input voltage variations. In order to achieve high performance despite system uncertainties, cascade control or current mode control is used which uses two first-order systems for the control implementation.

Cascade control deals with current and voltage dynamics separately, and the controller design is composed of inner-loop current control and outer-loop voltage control, in a cascade manner. For example, a backstepping approach was employed for systematic control design. Zhong and Hornik proposed a cascaded current-voltage control method using the H_∞ control strategy. An adaptive controller was proposed to reduce the output voltage ripple caused by disturbances in the input voltage. Digital implementation of a two-loop controller having sliding-mode current control and proportional-integral (PI) voltage control was developed.

This paper presents a new cascade controller for dc/dc boost converters. We have used integral-proportional (IP) control for the outer-loop and PI control for the inner-loop to produce the desired control of the nominal closed-loop system. However, because the dc/dc boost converter is a highly nonlinear system, the IP-PI cascade control scheme, based on a linearized model, may not achieve the desired performance in the presence of parametric uncertainties and input voltage variations. In order to provide a robust transient performance against various uncertainties, nested reduced-order PIOs are incorporated with the predesigned cascade control structure.

In this paper, the theoretical analysis along with the simulation of boost converter with existing controllers was conducted under three different cases: reference input change, load change, and input dc voltage variation by using a programmable dc power source.

The contribution of this paper is as follows.

- 1) A cascade control approach is presented for a dc/dc boost converter by combining an IP–PI cascade control and nested reduced-order PIOs to maintain desirable performance of the nominal closed-loop system using the predesigned cascade controller without accounting for various uncertainties.
- 2) Theoretical analysis is performed on the performance of the closed-loop converter system with the PIOs, which confirms the desired approximation of the augmented system to the nominal closed-loop system without accounting for the uncertainties.
- 3) Bode plot analysis of the circuit is performed under reference input change, load change, and input dc voltage variation by using a programmable dc power source.
- 4) Hardware circuit was implemented and it is tested using DC battery of 12V and solar panel as inputs.

3.1. Cascade control for nominal performance

3.1.1 Linearized model of Boost Converter

This paper deals with the output voltage regulation problem of the dc/dc boost converter shown in Fig.1. The model accounts for a parasitic resistance R_L of the inductor and a current-sensing resistor R_s to represent unavoidable voltage drops. While other parasitic elements can be included as in [8], the model of Fig.1 is a result of the trade-off between exact model description and controller design simplicity.

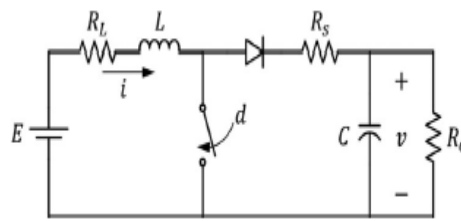


Figure1. DC/DC boost converter model with R_L and R_s

The mathematical model of Fig1. is described by

$$\frac{di}{dt} = -\frac{R_L}{L}i - (1-d)\left(\frac{R_s}{L}i + \frac{1}{L}v\right) + \frac{E}{L} \quad \text{---(2a)}$$

$$\frac{dv}{dt} = (1-d)\frac{1}{C}i - \frac{1}{R_o C}v \quad \text{---(2b)}$$

where 'i' is the inductor current, v is the output voltage, and E is the dc input. The duty ratio d ($0 \leq d \leq 1$), defined as the ratio of the on duration of the switch to the switching time period T_s , controls the output voltage by adjusting the on duration [9]. The parameters L, C, and R_o denote the inductance, capacitance, and load resistance, respectively. All parameters, including the input voltage E, are assumed to be uncertain and/or slowly varying with known nominal values.

When the desired output voltage is V_d ($V_d > E$), the equilibrium values of i and d are given by

$$I = \frac{V_d}{(1-D)R_o} \quad \text{---(3a)}$$

$$D = 1 - \frac{1}{2} \left[\frac{E}{V_d} - \frac{R_s}{R_o} + \sqrt{\left(\frac{E}{V_d} - \frac{R_s}{R_o}\right)^2 - \frac{4R_L}{R_o}} \right] \quad \text{---(3b)}$$

The Jacobian linearization of (2) at the equilibrium point $(i, v, d) = (I, V_d, D)$ yields

$$\dot{x}_1 = -\frac{R_1}{L}x_1 + \frac{V_1}{L}\left(u - \gamma_1 \frac{1-D}{V_1}x_2 - f_c\right)$$

$$\dot{x}_2 = -\frac{1}{R_0C}x_2 + \frac{1-D}{C}\left(x_1 - \gamma_2 \frac{I}{1-D}u - f_v\right)$$

----(4b)

where $x = [i, v - V_d]^T$, $u = d - D$, $R_1 = R_L + R_s(1 - D)$, $V_1 = R_s I + V_d$, and $\gamma_1 = \gamma_2 = 1$; f_c and f_v represent equivalent lumped disturbances, including unmodeled dynamics. Fig.2 describes the block diagram of system (4).

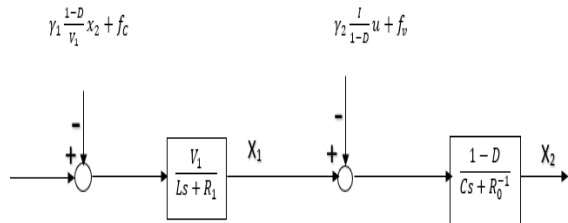


Figure2. Block diagram of the linearized system

3.1.2. Ideal Cascade Control Using IP and PI Controllers

When $f_c = f_v = 0$ in Fig. 2, the transfer function from u to x_2 is given by

$$G(s) = \frac{-\frac{\gamma_2 I}{C} \left(s - \frac{(1-D)V_1}{r_2 L I} + \frac{R_1}{L} \right)}{\left(s + \frac{R_1}{L} \right) \left(s + \frac{1}{R_0 C} \right) + \gamma_1 \frac{(1-D)^2}{LC}}$$

----(5)

where the zero is unstable for practical circuit parameters[9]. It is noted that the transfer function can be a cascade of two first-order minimum phase systems if $\gamma_1 = \gamma_2 = 0$. In order to obtain desirable nominal performance of a closed-loop converter system, this paper presents a cascade controller for (5) without accounting for the disturbances f_c and f_v . The controller comprises two parts: 1) an outer (voltage-loop) IP controller; and 2) an inner (current-loop) PI controller. The two conventional controllers are depicted in Fig.3[4]. The closed-loop transfer function with the IP controller does not have an additional zero, which is often helpful for reducing the overshoot of the output response.

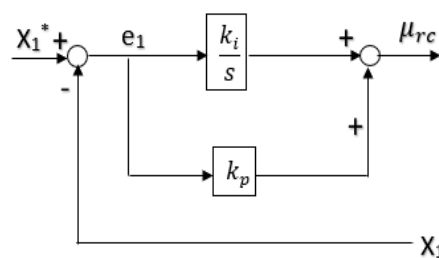


Figure3 (a). Two conventional controllers. (a) PI controller

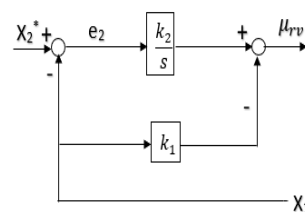


Figure3(b). IP controller

The outer-loop IP controller generates the reference x_1^* for the inner loop. Following the back-stepping approach [10], the state x_1 in (4b) is first assumed to be a virtual control input x_1^* for the voltage loop. When x_2^* is the desired value of x_2 , the IP controller with a feedforward cancellation term is

$$: x_1^* = -k_1 x_2 + k_2 \int_0^t e_2 dt + \frac{1}{1-D} u \quad \text{---- (6)}$$

where $e_2 = x_2^* - x_2$, and k_1 and k_2 are the control gains.

The closed-loop characteristic polynomial is given by

$$: s^2 + \left(\frac{1}{R_0 C} + \frac{1-D}{C} k_1 \right) s + \frac{1-D}{C} k_2 \quad \text{---- (7)}$$

$$:= s^2 + 2\zeta_v \omega_v s + \omega_v^2$$

where ζ_v and ω_v are the design parameters. ---- (8)

The inner-loop PI controller adjusts the duty ratio to make the state x_1 track the reference x_1^* . The PI controller design is based on the technical optimum scheme, and use of the controller results in a simple first-order closed-loop system. The PI controller with a feedforward term is given by

$$: u = \frac{\omega_c L}{V_1} e_1 + \frac{\omega_c R_1}{V_1} \int_0^t e_1 dt + \frac{1-D}{V_1} x_2$$

where $e_1 = x_1^* - x_1$, and ω_c is the bandwidth of the current-loop system. After a stable pole/zero cancellation, the closed-loop transfer function is obtained as

$$: X_1(s) = \frac{\omega_c}{s + \omega_c} X_1^*(s)$$

where x_1 is the Laplace transform of x_1 . Choosing the bandwidth ω_c as a sufficiently large value, it can be obtained that $x_1 \approx x_1^*$. This implies that the control problem for (4) can be solved by (9) with (6) when $f_c = f_v = 0$.

Although two integrators are employed in the IP-PI cascade control scheme, nominal performance could not be achieved under the combined presence of parametric uncertainty, input voltage variation, and disturbances f_c and f_v . Performance degradation of the real closed-loop system is compensated via nested reduced-order PIOs.

3.1.3. Robust performance via nested reduced-order PIOs

Since this approach deals with the two first-order systems (4) separately but in the same manner, this section first considers the representative first-order system of Fig4(a), associated with the real uncertain parameters a_r and b_r , and the disturbance f . The actual parameters a_r and b_r and so on corresponding to Fig (4a) and Fig(4b) are listed in table 1.

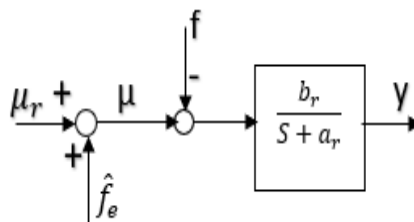


Figure4. Performance recovery using PIO.

(a) Feedforward compensation using f_e

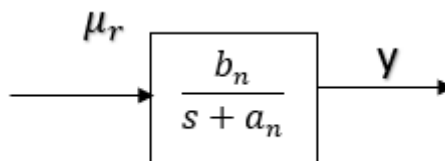


Figure4(b). Nominal system

The signal μ_r can be treated as the reference in Fig 4(a), but it will become the signals μ_{rc} and μ_{rv} as shown in Fig.5.

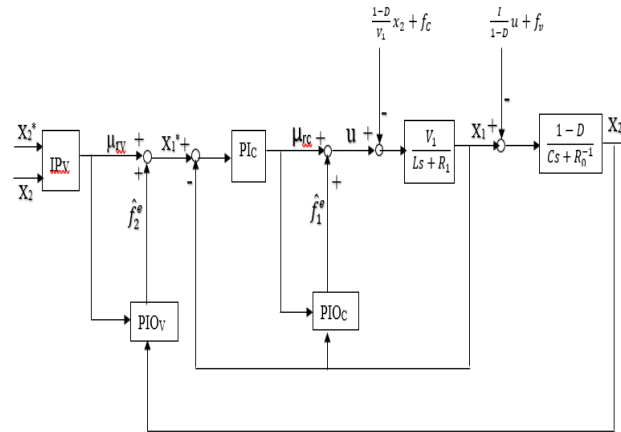


Figure5. Cascade IP–PI control using nested reduced-order PI observers

The objective of the reduced-order PIO in this section is to design \hat{f}_e so that the system of Fig.4 (a) behaves in the same way as the system of Fig.4(b) after the fast transient of \hat{f}_e . a_n and b_n are the nominal values of a_r and b_r , respectively.

The system of Fig.4 (a) is described by

$$\dot{y} = -a_r y + b_r (\mu - f) \quad \text{---(11)}$$

where $a_r > 0$ and $b_r > 0$ (see Table1).

TABLE1. Converter Parameters for the Observer Design

PARAMETER	PIO _c (CURRENT LOOP)	PIO _v (VOLTAGE LOOP)
$a_n (a_r)$	R_1 / L	$1 / R_0 C$
$b_n (b_r)$	V_1 / L	$(1 - D) / C$
f	$(1 - D) x_2 / V_1 + f_c$	$(I u) / (1 - D) + f_v$
\hat{f}_e	\hat{f}_1^e	\hat{f}_2^e
μ	u	x_1
μ_r	μ_{rc}	μ_{rv}
y	x_1	x_2

In order to account for parametric uncertainties, (11) is rewritten as

$$\dot{y} = -a_n y + b_n (\mu - f_e) \quad \text{---(12a)}$$

$$f_e = (\tilde{a} y - \tilde{b} \mu + b_r f) / b_n \quad \text{---(12b)}$$

where $\tilde{a} = a_r - a_n$ and $\tilde{b} = b_r - b_n$.

When $h := f_c$, the following system is considered as the model of (11):

$$\begin{bmatrix} \dot{y} \\ \dot{f}_e \end{bmatrix} = \begin{bmatrix} -a_n & -b_n \\ 0 & 0 \end{bmatrix} \begin{bmatrix} y \\ f_e \end{bmatrix} + \begin{bmatrix} b_n \\ 0 \end{bmatrix} \mu + \begin{bmatrix} 0 \\ h \end{bmatrix} \quad \text{---(13)}$$

When the disturbance f_e is supposed to vary slowly relative to the observer dynamics, the reduced-order observer can be designed to estimate the disturbance as follows:

$$\hat{f}_e = l(f_e - \hat{f}_e) = l(-\dot{y} - a_n y + b_n \mu - b_n \hat{f}_e) / b_n \quad \text{---(14)}$$

where the observer gain $l > 0$. In order to implement (4.13) without using \dot{y} , a new variable ξ is defined as

$$\begin{aligned} \xi &= \hat{f}_e + \frac{l}{b_n} y \\ \text{Or: } \hat{f}_e &= \xi - \frac{l}{b_n} y \end{aligned}$$

----(15)

using (14), the reduced-order PIO is rewritten as

$$: \dot{\xi} = -l\xi + \frac{l}{b_n}(-a_n - l)y + l\mu = -l\frac{a_n}{b_n}y + l\mu_r \quad \text{----(16)}$$

with $\mu = \mu_r + \hat{f}_e$, as shown in Fig4(a).

The robustness analysis of the augmented system (11) with (14) was provided in [7] using a Lyapunov function approach and singular perturbation theory. For subsequent unified analysis, an enhanced Lyapunov function approach by using the boundedness of h. substituting (11) and $\mu = \mu_r + \hat{f}_e$ into (14) yields

$$: \dot{\hat{f}}_e = l(a_r y - b_r(\mu_r + \hat{f}_e - f) - a_n y + b_n \mu_r) / b_n \quad \text{----(17)}$$

when the observer gain l is sufficiently large, the systems described by (11) and (17) can be written in the standard singular perturbation form as follows:

$$: \dot{y} = -a_r y + b_r(\mu_r + \hat{f}_e - f) \quad \text{----(18a)}$$

$$: \epsilon \dot{\hat{f}}_e = \frac{a_r}{b_n} y - \frac{b_r}{b_n}(\mu_r + \hat{f}_e - f) - \frac{a_n}{b_n} y + \mu_r \quad \text{----(18b)}$$

where $\epsilon=1/l$. According to the singular perturbation analysis, the variables y, μ_r , and f in (18) are regarded as the slow variables, whereas the state \hat{f}_e stable.

Since all the parameters are positive, system (18) is stable. Moreover, the boundary-layer system (18b) is also stable and the quasi-steady-state solution \hat{f}_e^e of (18b) satisfies

$$: -a_r y + (b_r(\mu_r + \hat{f}_e^e - f)) = -a_n y + b_n \mu_r \quad \text{----(19)}$$

Therefore, in the quasi-steady-state, (18) becomes

$$: \dot{y} = -a_n y + b_n \mu_r \quad \text{----(20)}$$

which describes the same system as the nominal system of Fig4(b). This implies that the nominal performance of Fig4(b) can be recovered by using the reduced-order PIO approach after the fast transient of \hat{f}_e in the presence of parametric uncertainties as well as the disturbance f.

The complete analysis on the performance recovery property of the reduced-order PIO can be relaxed by using multiple integrals of the estimation error as in [11],[12].

Since the error \tilde{y} between the real system and the nominal system becomes arbitrarily small, the control input μ_r in Fig4(a) can be designed without accounting for parametric uncertainties and the disturbance as in Fig4(b).

Motivated by the nominal performance recovery property, the reduced-order PIO (15), (16) is incorporated with the predesigned controller to maintain the desired dynamic performance of the nominal closed-loop system. Substituting $\mu = \mu_{rc} + \hat{f}_1^e$ into (4a), as shown in Fig5, the current-loop equation is rewritten as

$$: \dot{x}_1 = -\frac{R_1}{L} x_1 + \frac{V_1}{L} (\mu_{rc} + \hat{f}_1^e - f_1) \quad \text{----(21)}$$

where $f_1 = (1 - D)x_2/V_1 + f_c$. The feedforward term in (9) has been included in the lumped disturbance f_1 .

As in (15) and (16), the PIO is designed by

$$: \hat{f}_1^e = \xi_c - l_c \frac{\bar{L}}{\bar{V}_1} x_1 \quad \text{----(22a)}$$

$$: \dot{\xi}_c = -l_c \frac{\bar{R}_1}{\bar{V}_1} x_1 + l_c \mu_{rc} \quad \text{----(22b)}$$

where $l_c > 0$. The parameters with bar symbols represent the nominal values. After a fast transient of \hat{f}_1^e , the real system (21) with (22) can be approximated by the nominal system:

$$: \dot{x}_1 = -\frac{\bar{R}_1}{\bar{L}} x_1 + \frac{\bar{V}_1}{\bar{L}} \mu_{rc} \quad \text{----(23)}$$

The inner-loop PI controller (PIc) is given by

$$: \mu_{rc} = \frac{\omega_c \bar{L}}{\bar{V}_1} e_1 + \frac{\omega_c \bar{R}_1}{\bar{V}_1} \int_0^t e_1 d\tau \quad \text{----(24)}$$

where $e_1 = x_1^* - x_1$ and $x_1^* = \mu_{rv} + \hat{f}_2^e$ (see Fig.5). The controller (24) has a simplified form without the feedforward term in (9) because the term has been compensated by PIc. Applying (24) to (23) yields the closed-loop system (10). This implies that the objective of the inner-loop control has been accomplished by $\mu_{rc} = \hat{f}_1^e$.

The cascaded connection of the closed-loop dynamics (10) and the voltage loop (4b) can be described by

$$: \dot{x}_2 = -\frac{1}{R_0 C} x_2 + \frac{1-D}{C} (x_1 - f_2) \quad \text{----(25a)}$$

$$\frac{1}{\omega_c} \dot{x}_1 = -x_1 + x_1^* \quad \text{----(25b)}$$

where $f_2 = (I_u)/(1-D) + f_v$. The cascaded system described by (25) is in the standard singular perturbation form when the current-loop bandwidth ω_c is sufficiently large. Since the boundary-layer system (25b) is stable, the quasi-steady state solution can be given by $x_1 = x_1^*$. Hence, it follows from $x_1^* = \mu_{rv} + \hat{f}_2^e$ that the system (25a) is represented in the quasisteady-state as

$$: \dot{x}_2 = -\frac{1}{R_0 C} x_2 + \frac{1-D}{C} (\mu_{rv} + \hat{f}_2^e - f_2) \quad \text{----(26)}$$

The PIO for constructing \hat{f}_2^e is given by

$$: \hat{f}_2^e = \xi_v - l_v \frac{\bar{C}}{1-\bar{D}} x_2 \quad \text{----(27a)}$$

$$: \dot{\xi}_v = -l_v \frac{1}{(1-\bar{D})R_0} x_2 + l_v \mu_{rv} \quad \text{----(27b)}$$

where $l_v > 0$. In the same way as the current loop, after a fast transient of \hat{f}_2^e , (26) with (27) can be approximated by

$$: \dot{x}_2 = -\frac{1}{R_0 \bar{C}} x_2 + \frac{1-\bar{D}}{\bar{C}} \mu_{rv} \quad \text{----(28)}$$

As the last step of the proposed controller design, the outer loop IP controller (IPv) is given by

$$\mu_{rv} = -k_1 x_2 + k_2 \int_0^t e_2 dt \quad \text{----(29)}$$

where $e_2 = x_2^* - x_2$, and k_1 and k_2 are the control gains. Since the characteristic polynomial of (28) and (29) is given by

$$s^2 + \left(\frac{1}{R_0 C} + \frac{1-D}{C} k_1 \right) s + \frac{1-D}{C} k_2 \quad \text{----(30a)}$$

$$= s^2 + 2\zeta_v \omega_v s + \omega_v^2 \quad \text{----(30b)}$$

the control objective of the outer loop can be achieved if ζ_v and ω_v (or, k_1 and k_2) are selected such that the polynomial (30) is Hurwitz.

If the observer gains l_v and l_c are sufficiently large, the PIOv and PIOc recover the nominal performance of the proposed IP–PI cascade controller without accounting for parametric uncertainties, input voltage variations, and unmodeled dynamics. It is suggested, for the controller design, to set $\omega_v < l_v < \omega_c < l_c$. Indeed, the nominal system recovery can be obtained when $l_c > \omega_c$, and $\omega_c > l_v$. Finally, by using the equation $\mu = \mu_{rc} + \hat{f}_1^e$ the control objective is accomplished by the proposed controller.

III. Stability analysis

4.1. Bode plot analysis

Bode plots are used for determining the relative stabilities of the given system.

The transfer functions of Boost converter as shown in Fig5 under various conditions are as follows:

1. Boost converter without any controllers:

$$G(s) = \frac{-4000[s - (1 - D) \cdot 947 \times 10^6 + 1270]}{(s + 1270)(s + 250) + (1 - D)^2}$$

----(31)

2. Boost Converter with PI & IP controllers:

$$G_C(s) = \frac{G(s) \cdot \left(s + \frac{k_i}{k_p} \right) k_p k_2}{(s^2 + k_1 k_2 s)}$$

----(32)

3. Boost converter with PI & IP controllers along with PI observers:

$$G_{PIO}(s) = G_C(s) \frac{(1 - D)}{C(s + 250)} \frac{0.378 \times 10^6}{(s + 1268.9)} \quad \text{----(33)}$$

4.2. Stability conditions of bode plots

Stability conditions are given below:

1. For Stable System: Both the margins should be positive or phase margin should be greater than the gain margin.
2. For Marginal Stable System: Both the margins should be zero or phase margin should be equal to the gain margin.
3. For Unstable System: If any of them is negative or phase margin should be less than the gain margin.

4.3. Analysis values

Calculation of gain margin (G.M) and phase margin (P.M) for different ‘D’ values are tabulated and is as shown in Table2.

TABLE2. Bode Plot Analysis Values

Duty Ratio ‘D’	Boost converter without controllers		Boost converter with PI-IP		Boost converter with PIO	
	G.M	P.M	G.M	P.M	G.M	P.M
0	0.3803	-2.4224	1.517×10^4	99.6208	0.013	177.579
0.2	0.3801	-2.6841	1.214×10^4	102.032	5.0474	38.7958
0.4	0.38	-3.0729	9.1178×10^3	106.063	3.7578	31.2948
0.6	0.3807	-3.7285	6.095×10^3	114.144	2.4546	20.8972
0.8	0.3801	-5.2287	3.093×10^3	130.323	1.1119	2.534
1	0.0625	-86.4162	Inf	74.5566	0.0123	178.898

From the above tabulation, it is observed that the boost converter with Proportional Integral Observers along with PI – IP controllers is more stable compared to the boost converter without controllers and also with PI & IP controllers and it occurs for duty cycle D = 0.8.

4.4. Bode plots for duty ratio D=0.8

Bode plots for the system shown in Fig.5 are as shown in Figs 6, 7, 8.

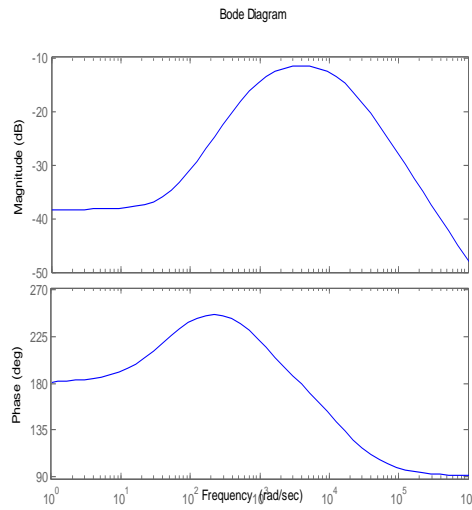


Figure6. Bode plot of Boost converter without controllers

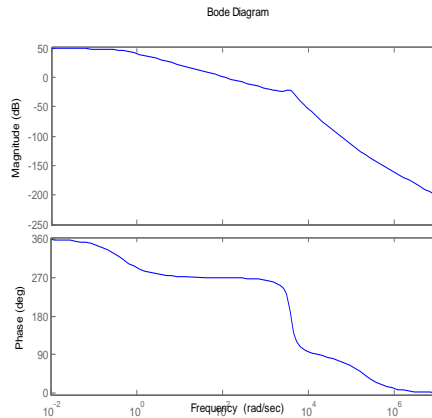


Figure7. Bode plot of Boost converter with PI -IP controllers

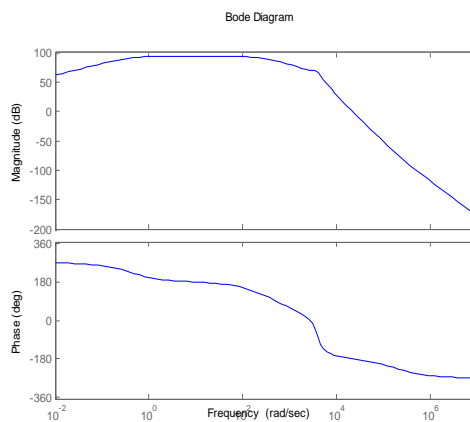


Figure8. Bode plot of Boost converter with PI -IP controllers & PIO

IV. Experimental results

The boost converter as shown in Fig. 5 was tested via MATLAB simulations under reference input change, load variation and input voltage variations. The performance tests were conducted for three cases:

- a) The desired voltage $V_d = 10$ V was changed to 10.2 V at $t = 0.2$ s; it was then returned to 10 V at $t = 0.21$ s and the same changes were applied at 0.6s and 0.61s respectively.
- b) The load resistance was varied from $R_o = 40.0 \Omega$ to $R_o = 20.0 \Omega$ by a toggle switch.
- c) The input voltage E was varied from 10 V to 20 V by a programmable dc power supply.

The results of computer simulations are as follows:

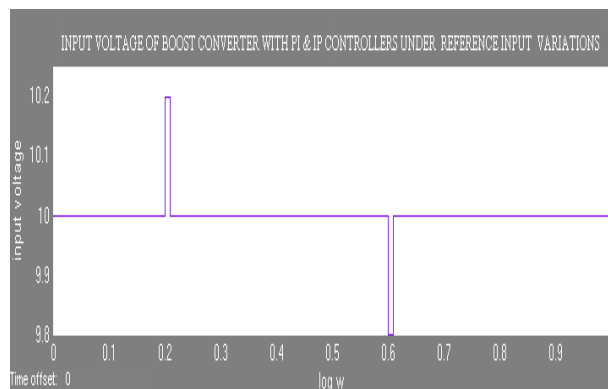


Figure9(a). Input voltage of boost converter with PI & IP controllers under reference input variations

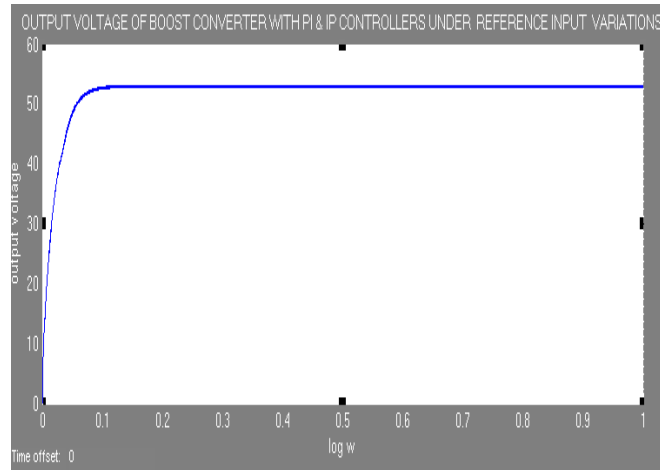


Figure9(b). Output voltage of boost converter with PI & IP controllers under reference input variations

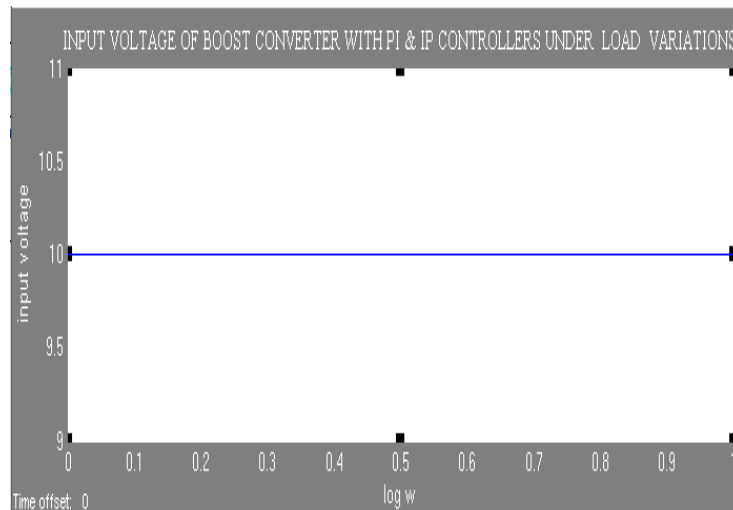


Figure10(a). Input voltage of boost converter with PI & IP controllers under load variations

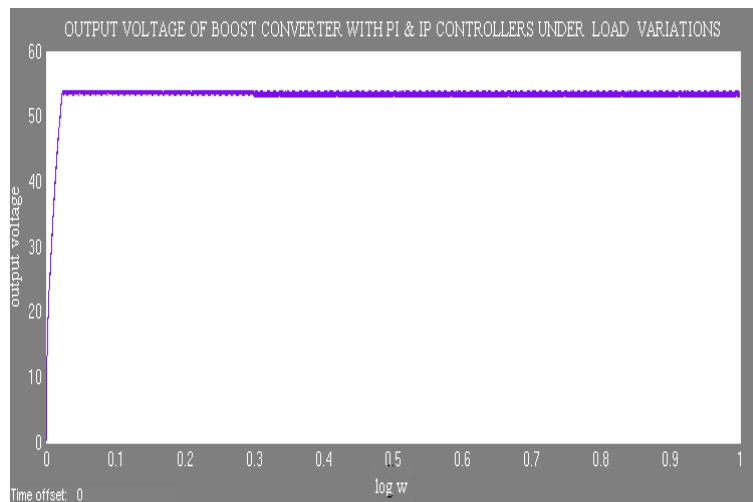


Figure10(b). Output voltage of boost converter with PI & IP controllers under load variations

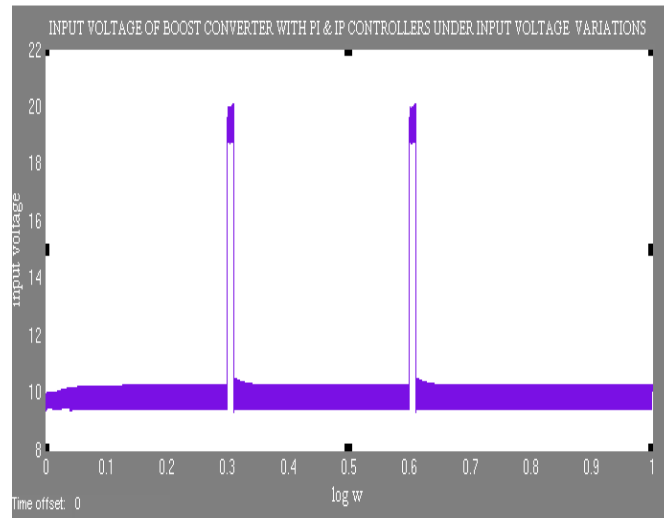


Figure11(a). Input voltage of boost converter with PI & IP controllers under input voltage variations

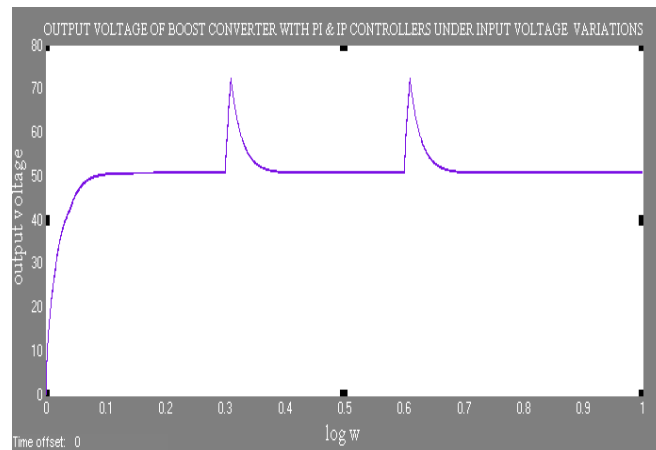


Figure11(b). Output voltage of boost converter with PI & IP controllers under input voltage variations

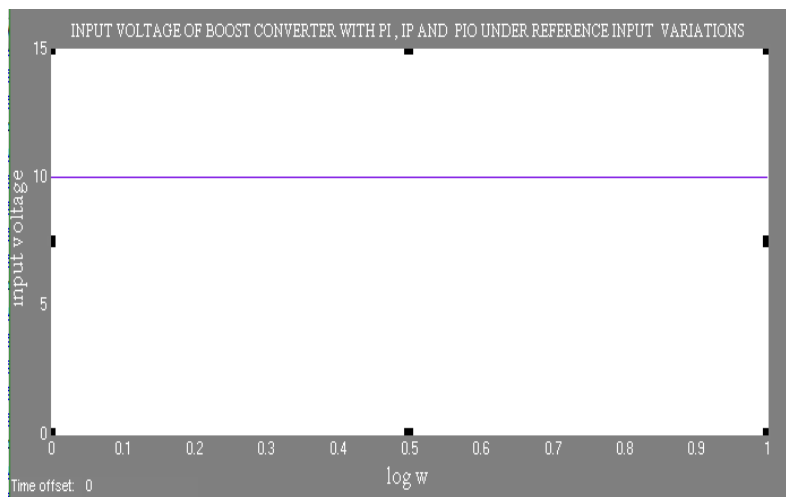


Figure12(a). Input voltage of boost converter with PI & IP controllers and PIO under reference input variations

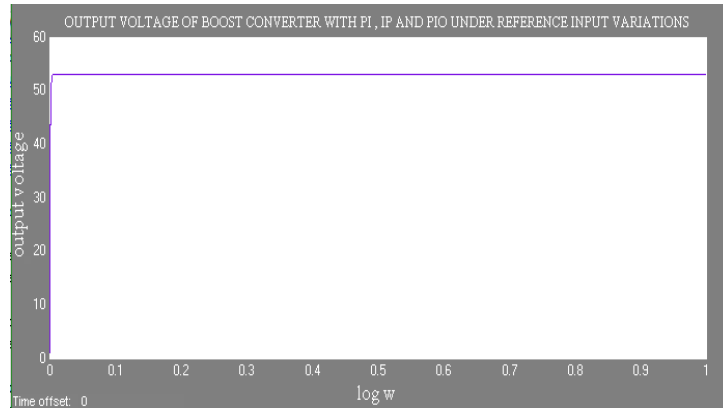


Figure12(b). Output voltage of boost converter with PI & IP controllers and PIO under reference input variations

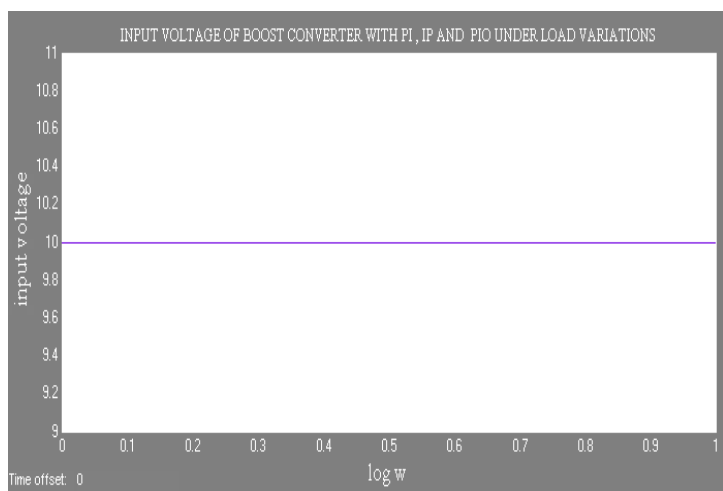


Figure13(a). Input voltage of boost converter with PI & IP controllers and PIO under load variations

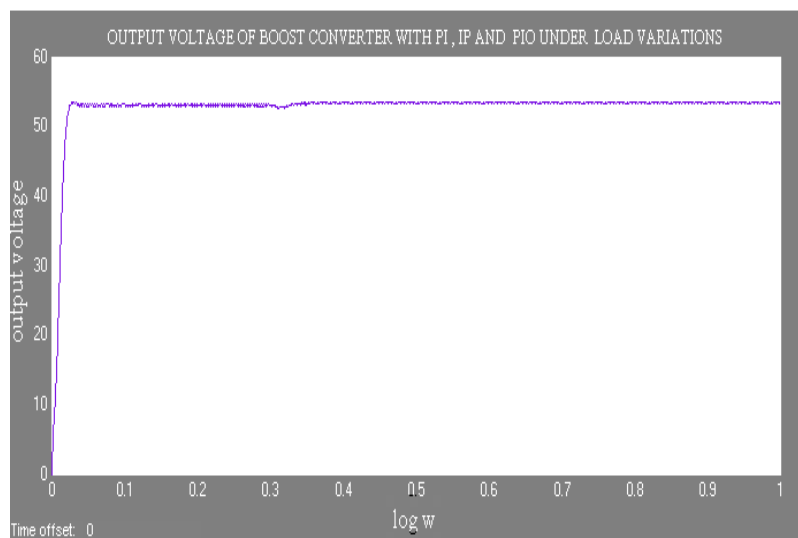


Figure13(b). Output voltage of boost converter with PI & IP controllers and PIO under load variations

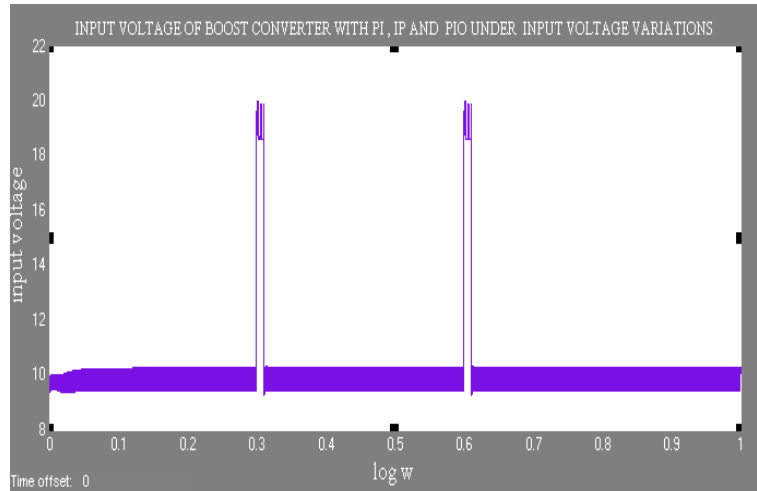


Figure14(a). Input voltage of boost converter with PI & IP controllers and PIO under input voltage variations

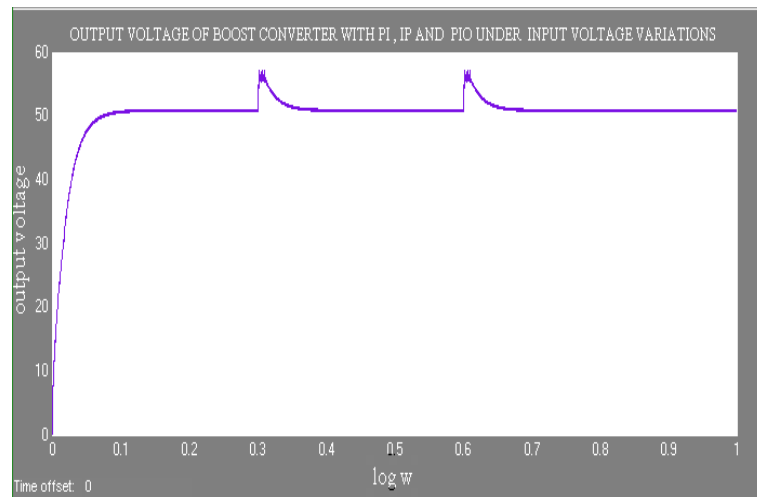


Figure14(b). Output voltage of boost converter with PI & IP controllers and PIO under input voltage variations

Experimental results in above Figs compared the boost converter with nested PIO along with PI – IP controllers and without PIOs from the simulation results. Owing to the measurement noise, the results show a little noisy response. The results of case a show that the system with PIOs almost preserved the nominal performance in the transient period. In the cases of b and c, the system with PIOs recovered the nominal performance after a short transient response. The results suggest that the proposed method using nested PIOs could be used effectively to maintain the desired dynamic performance against various uncertainties of the boost converter.

V. Hardware implementation of boost converter

The boost converter was designed using various components like 555 timer, power MOSFET and potentiometer. The 555 timer was used to generate the necessary triggering for the MOSFET as 555 timer can produce stable time delays. The hardware implementation circuit diagram and its output when connected to DC battery of 12 V and to solar panel are represented in this paper.

Fig15. shows the hardware representation of boost converter in which the conventional switch operation was performed using power MOSFET. The necessary pulse signals for the MOSFET was applied by using 555 timer.

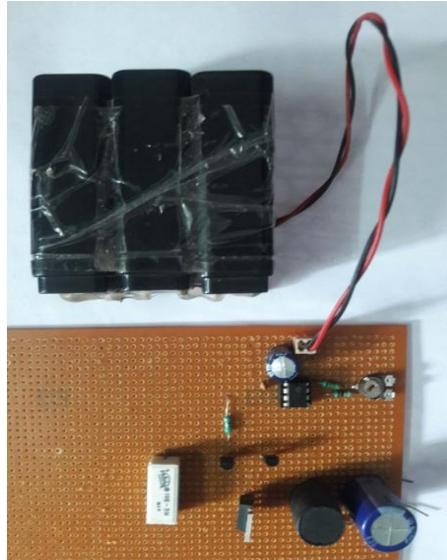


Figure15. Hardware implementation of boost converter

Fig 16. shows the output of boost converter when it was connected to DC supply.



Figure16. Output of boost converter when

it was connected to DC supply

Fig. 17 (a) & (b) shows the input given to the circuit and output of boost converter when the input was connected to solar panel.

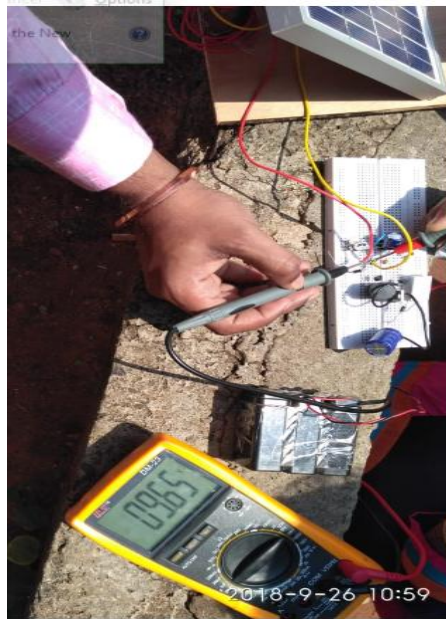


Figure 17(a). Input of the boost converter circuit when the input was connected to solar panel



Figure 17(b). Output of boost converter circuit when the input was given by solar panel

From the above inputs and outputs, we can observe that the boost converter which was designed using hardware components steps up its voltage level to almost nearer to 2.5 times the input voltage.

VI. Conclusion

This paper has presented a robust controller for regulating the output voltage of a dc/dc boost converter. In order to obtain a nominal desirable dynamic response, the cascaded PI and IP controllers were designed for a linearized model without accounting for the uncertainties. The predesigned cascade controller was combined with nested reduced-order PIOs to maintain the desired voltage regulation performance under various uncertainties. Theoretical analysis based on singular perturbation theory and a Lyapunov function approach confirmed the approximation of the augmented closed-loop system to the nominal closed-loop system.

Computer simulations showed that the system could be effectively used to handle significant plant uncertainties, such as load change, parametric uncertainties, and input voltage variations.

The stability analysis of the system was performed using bode-plot analysis and tabulated the gain margin and phase margin values of the system for different duty ratios. It was observed that the system was more stable at $D = 0.8$.

The boost converter was implemented using hardware components and obtained the output voltage approximately equal to 2.5 times the input voltage when the input was given using DC 12V battery and also by using solar panel.

References

- [1]. Design of Monolithic Step-Up DC-DC Converters with On-Chip Inductors by Ayaz Hasan
- [2]. Multi Loop Digital Control for Active Filter and DC/DC Converter Kristoffer Anderson, Christian M. Artensson
- [3]. Proportional-Integral-Observer: A brief survey with special attention to the actual methods using ACC Benchmark F. Bakhshande _ D. Soffker _ Chair of Dynamics and Control University of Duisburg-Essen, Duisburg, Germany
- [4]. P - I and I - P Controllers In A Closed Loop For DC Motor Drives F. I. Ahmed, A. M. El-Tobshy Professor of Power Electronics, A. A. Mahfouz Assistant Professor of Power Electronics, M. M. S. Ibrahim Ph.D. Candidate of Power Electronics , Faculty of Engineering, Cairo University ,Cairo, EGYPT
- [5]. www.netrino.com – Introduction to Pulse Width Modulation (PWM)
- [6]. Regulation of a DC/DC Boost Converter Under Parametric Uncertainty and Input Voltage Variation Using Nested Reduced-Order PI Observers In Hyuk Kim, Student Member, IEEE, and Young Ik Son, Member, IEEE
- [7]. Y. I. Son, I. H. Kim, D. S. Choi, and H. Shim, “Robust cascade control of electric motor drives using dual reduced-order PI observer,” *IEEE Trans. Ind. Electron.*, vol. 62, no. 6, pp. 3672–3682, Jun. 2015.
- [8]. A. Leon-Masich, H. Valderrama-Blavi, J. M. Bosque-Moncusí, J. Maixé-Altés, and L. Martínez-Salamero, “Sliding-mode-control-based boost converter for high-voltage–low-power applications,” *IEEE Trans. Ind. Electron.*, vol. 62, no. 1, pp. 229–237, Jan. 2015
- [9]. N. Mohan, T. M. Undeland, and W. P. Robbins, *Power Electronics: Converters, Applications, and Design*. Hoboken, NJ, USA: Wiley, 2003.
- [10]. H. K. Khalil, *Nonlinear Systems*. Englewood Cliffs, NJ, USA: Prentice-Hall, 2002.
- [11]. G.-P. Jiang, S.-P. Wang, and W.-Z. Song, “Design of observer with integrators for linear systems with unknown input disturbances,” *Electron. Lett.*, vol. 36, no. 13, pp. 1168–1169, Jun. 2000.
- [12]. K.-S. Kim, K.-H. Rew, and S. Kim, “Disturbance observer for estimating higher order disturbances in time series expansion,” *IEEE Trans. Autom. Control*, vol. 55, no. 8, pp. 1905–1911, Aug. 2010.

G.V.S.Lakshmi "Design of Boost Converter with Pi & Ip Controllers And Pi Observer"
International Journal Of Engineering Science Invention (IJESI), Vol. 08, No. 02, 2019,
Pp 63-80